Compatibility Studies of Poly(styrene) and Poly(vinyl acetate) Blends Using Electrostatic Force Microscopy

Mohammed M. Kummali,[1,2] Gustavo A. Schwartz,[2] Angel Alegría,[1,2] Richard Arinero,[3] Juan Colmenero[1,2,4]

[1]Departamento de Física de Materiales UPV/EHU, Fac. de Química, 20080 San Sebastián, Spain

[2]Centro de Física de Materiales CSIC-UPV/EHU, Paseo Manuel de Lardizabal 5, 20018 San Sebastián, Spain

[3]Institut d' Electronique du Sud (IES), Universitè Montpellier II, 34095 Montpellier Cedex, France

[4]Donostia International Physics Center, Paseo Manuel de Lardizabal 4, 20018 San Sebastián, Spain

Correspondence to: M. M. Kummali (E-mail: mohammedmusthafa.kummali@ehu.es)

Received 2 May 2011; revised 6 June 2011; accepted 6 June 2011; published online
DOI: 10.1002/polb.22301

ABSTRACT: The effect of thermal treatment on the phase separation process of the components of a polymer blend was investigated using electrostatic force microscopy (EFM). EFM technique is an advance on conventional atomic force microscopy, which enables us to measure locally the dielectric properties of the samples under investigation providing compositional information. In this work, we studied the phase separation process of the polymer blend thin films made of poly(styrene) and poly(vinyl acetate) (PS/PVAc) (75/25 weight fraction). The samples were subjected to different thermal treatments. It was found that at low annealing temperature, PVAc forms many small islands within PS matrix. As the annealing temperature increases, the number of PVAc islands decreases with an increase in the size of the islands. These islands take spherical-like shape when annealed at a temperature well above the glass transition temperatures of both the component polymers. Despite these morphological/topographical changes, EFM images evidence that there is no interdiffusion which was further confirmed by quantitatively measuring the value of the dielectric permittivity across the interphase. © 2011 Wiley Periodicals, Inc. J Polym Sci Part B: Polym Phys 000: 000–000, 2011

KEYWORDS: compatibility; electrostatic force microscopy; local dielectric mapping; polystyrene; poly(vinyl acetate)

INTRODUCTION Blending of polymers provides an attractive way to combine properties of blend components and thus generate new materials with an optimized performance.[1,2] Determination of the compatibility in polymer blends is of considerable importance because manifestation of their superior properties depends on the compatibility or miscibility of homopolymers at molecular level.[3] In certain cases, nanostructured materials can be obtained by means of nanophase segregation of the components of the blend. Being a key factor in the tailoring of polymer blends, compatibility can be determined theoretically as well as experimentally.[4–8] Compatibility/phase segregation studies of polymer blends having significant differences in the properties of the component polymers have attracted great attention. Blends made of polystyrene (PS) and poly(vinyl acetate) (PVAc) are among such blends in which the thermal and dielectric properties of both components vary significantly.

Compatibility and phase structure of polymer blends can be investigated by different techniques. However, most of them fail to give detailed information about the miscibility behavior at local scale. Hence, it is desirable to develop simple and accurate techniques to study the phase structure of polymer blends at nanoscale. Common techniques such as confocal microscopy, transmission electron microscopy (TEM), scanning electron microscopy, and atomic force microscopy (AFM) are being used to study the complex phase structure of polymer blends at nanoscale. All of these techniques make use of certain characteristic features of the component polymers, such as density, elasticity, conductivity, mechanical strength, and so forth, to study the phase structure. For example, TEM works based on the electron density of states. Polymers having different electron density of states respond differently with transmitted electrons, and, thus, TEM can be used to study the phase separation process only in case where the electron density of the polymers varies considerably. Moreover, the high-energy electrons in TEM can damage the polymer films, and the specimen preparation process is also potentially destructive and complicated. AFM can also be used to study the phase separation of two polymers on the ground that mechanical properties of polymers

vary differently with variations in temperature. It mainly uses topographic features to study the process of phase separation, but, in some cases, it would not be adequate to distinguish the component features. Moreover, it might be deceptive to consider the topography alone. Recently, a new AFM-based approach to measure the local dielectric properties of polymer thin films has been developed.[9,10] This, electrostatic force microscopy (EFM), allows measuring the dielectric properties with a lateral resolution of typically a few tens of nanometers with good sensitivity. Thus, EFM together with conventional AFM could be used to study the polymer blend structure more effectively. In addition, the dielectric contrast can be improved by properly tuning the temperature and/or frequency of the applied voltage.[11]

The compatibility of PS with PVAc has been a long debate issue. Previous works[12–14] performed on PS/PVAc blends suggest all three possibilities. Some researchers, Elashmawi et al.,[12] propose that these two polymers are fully miscible. In this case, the samples were prepared using acetone as the common solvent. The blends were subjected to a thermal treatment of 50 °C for 3 days, before been analyzed using FTIR, DSC, and UV/IR spectroscopy techniques. A second group of researchers, Rawal et al.,[13] states that the miscibility is only partial. They mixed the polymers in methyl ethyl ketone (MEK) and then subjected the blends to a thermal treatment of 70 °C for a day. In this case, viscometry and FTIR spectroscopy were used to characterize the miscibility. A third group of researchers, Mamza et al.,[14] found that the PS and PVAc are two immiscible polymers. In their work, they used different solvents namely toluene, MEK, and tetrahydrofuran (THF) for mixing the two polymers, but the followed thermal treatment was not indicated. They used density and viscometry techniques for characterization. The immiscibility nature of the two polymers was again confirmed by Riedel et al.[10,20] by quantifying locally the dielectric permittivity of very thin films prepared by spin coating a 5% toluene solution, annealed at 120 °C under vacuum for 2 h. All these results evidence the importance of solvents used and also the annealing conditions on the obtained conclusions. However, the intrinsic miscibility of any binary polymer system would require achieving the more favorable equilibrium state, which implies removing completely the solvent and using a relatively high annealing temperature.

The recently developed dielectric characterization technique based on EFM opens the possibility of investigating the compatibility of PS/PVAc system as the annealing temperature of the sample is modified. Thus, in this work, we study the degree of compatibility of PS/PVAc polymer blends in the ratio 75/25 (weight fraction) prepared using different thermal treatments. We mapped the dielectric contrast of the samples in addition to the more standard topography and AFM phase images. The quantification of the local dielectric permittivity in selected spots allows us to determine the composition of the segregated phases confirming that the phase segregation is improved when higher temperature treatments are used.

EXPERIMENTAL

Sample Preparation

Blends made of PS ($M_w = 70{,}950$) and PVAc ($M_w = 83{,}000$) in the ratio 75/25 were prepared. The macroscopic dielectric behavior of these polymers is well characterized in the literature.[15–18] In particular, PS/PVAc is a polymer blend which has been investigated for a long time. Moreover, this system is particularly suitable for using EFM technique because of the high dielectric contrasts between both components, as dielectric constant of PVAc at temperatures slightly above glass transition (ca. 60 °C) is about 8 whereas that of PS is close to 2.8. The polymers were mixed in toluene at a 4% solution concentration. This solution was then spin coated over thin glass plates, previously sputtered with gold, to get thin films of about 0.2 μm. These were then subjected to different thermal treatments. All the samples were kept in oven under vacuum for a day, at 40, 80, and 160 °C. They were coded as A to C, respectively.

EFM Measurements

The EFM work was accomplished using a Veeco di Multimode V AFM from Digital Instruments, with a NanoScope V Controller. The topography (height) of the sample and the cantilever phase images were obtained by performing standard tapping mode AFM and the dielectric contrast images were obtained by using EFM with double pass method.[19] In double pass method, the topographical features are acquired during the first scan, and during the second scan, the tip is kept at an average height ("lift height") above the sample surface without touching it. In this scan, a voltage of typically 5 V is applied to the tip. The change in the resonant frequency of the cantilever is then recorded while the cantilever scans across the sample. This change in resonance frequency is related to the applied voltage through the capacitance of the system (formed by the sample and the tip) as

$$\frac{\Delta f_0}{f_0} = \frac{-1}{4k_c}\frac{\partial^2 C}{\partial z^2}V^2\mathrm{dc} \tag{1}$$

$$\Delta f_0 = -a_{\Delta f_0}(z)V^2\mathrm{dc} \tag{2}$$

where,

$$a_{\Delta f_0}(z) = \frac{f_0}{4k_c}\frac{\partial^2 C}{\partial z^2} \tag{3}$$

is a parabolic coefficient. As capacitance C is a function of ε, the change in it can be mapped keeping all other parameters constant. For the quantitative analysis of the local dielectric permittivity, the change in resonance frequency of the cantilever was plotted against the applied voltages so as to confirm the parabolic profile (eq 2). This was then repeated for several tip-sample distances. Coefficients of the parabolas, thus, obtained as a function of tip-sample distance were compared with those extracted by using the so-called equivalent charge method (ECM)[9,10] for different permittivity values. This is shown in Figure 1. All the measurements were performed both at room temperature and at 60 °C, the

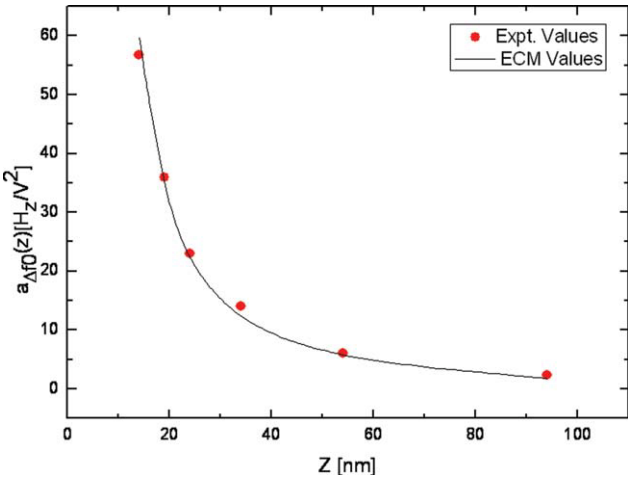

FIGURE 1 Coefficients of the parabola ($a_{\Delta f0}$) are plotted as a function of tip-sample distance. The red points correspond to the experimentally determined values which are then fitted using ECM (solid line). [Color figure can be viewed in the online issue, which is available at wileyonlinelibrary.com.]

latter being above the glass transition temperature of PVAc ($T_g = 38$ °C) enhances its dielectric constant.

RESULTS AND DISCUSSIONS

Figure 2 shows a typical topographic image of sample A (subjected to a thermal treatment of 40 °C) scanned in an area of 5 × 5 μm^2. In this figure, we can observe many island-like structures. This suggests that the polymers are phase separated to form domains as reported in previous works.[20,21] In this case, the domain diameter is typically of the order of a micrometer, which is in close agreement with that obtained for Magonov et al.[21] for the same blend.

Standard AFM gives the detailed information about the topographical features and the mechanical phase shift imaging of the sample under investigation (as shown in Fig. 3). In phase-mode imaging, the phase shift of the oscillating cantilever relative to the driving signal is measured. This phase shift can be correlated with specific mechanical properties which affect the tip/sample interaction.[23] Phase imaging has been useful to differentiate between component phases of composite materials if the mechanical properties of the components vary considerably.[24] Figure 3(b) represents phase-mode imaging while the cantilever sweeps across the sample. Here, the two phases (phases corresponding to the matrix and the islands) have almost the same shift. This is expected as both components are below their respective glass transition temperatures and thus have almost similar mechanical properties at room temperature (25 °C).

Figure 4 shows the mechanical phase image and a profile drawn across an island at 60 °C. This graph also shows a poor mechanical phase contrasts, showing that the mechanical properties of both phases are not sufficiently distinct at 60 °C. This suggests that the mechanical phase imaging is most likely to be affected by topography.

If the polymer components of a blend differ in their dielectric properties, then dielectric contrast mapping of the sample can provide compositional information even if their mechanical properties are similar. Moreover, the dielectric contrast mapping is not only determined by the very surface of the sample but also it probes a substantial region below the surface. Dielectric contrast mapping of the sample (sample A) was thus made both at room temperature and at 60 °C and is shown in Figure 5 along with profiles across islands. The profile drawn at room temperature is more noisy and the seperation between the two phases is less clear than that of 60 °C. This is because at room temperature the dielectric constant values of both phases are close to each other, as the permenant dipole orientational contributions to the permittivity of PVAc is not active (dipoles are frozen). On the contrary, at 60 °C, the dielectric constant of PVAc markedly increases (from about 3 at room temperature to about 8 at 60 °C). Thus, the high contrast of the image recorded at 60 °C, indicating greatly different values of dielectric constants, particularly the dielectric constants of the islands are significantly larger (higher frequency shift) than that of the matrix, suggests that the islands are composed mainly of PVAc and the matrix mainly of PS.

To quantify the composition of the phases, we determined the local dielectric permittivity, first at room temperature and then at 60 °C. Local dielectric permittivity at three distinct characteristic points were determined by performing

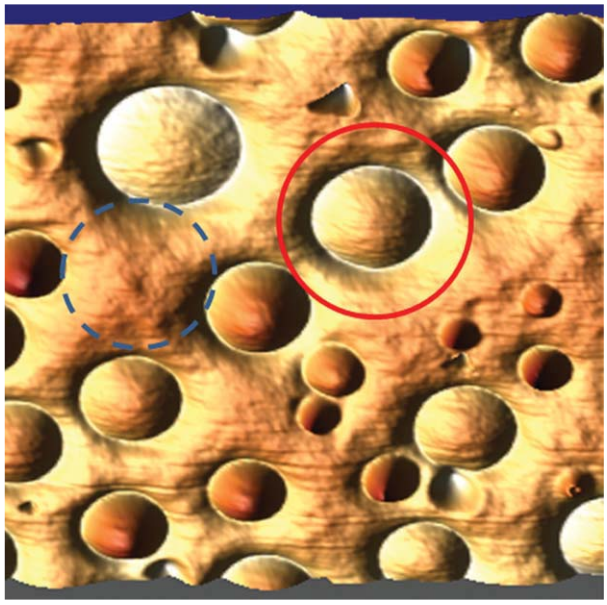

FIGURE 2 Three-dimensional (3D) topography image of sample A (subjected to a heat treatment of 40 °C). Measurements to determine the local dielectric permittivity were done on three distinct characteristic points viz. at the center of the island (marked red), at a point in between the center and the border of the island, and on the matrix (blue dashed line; Color online). Figures were processed using WSxM.[22] [Color figure can be viewed in the online issue, which is available at wileyonlinelibrary.com.]

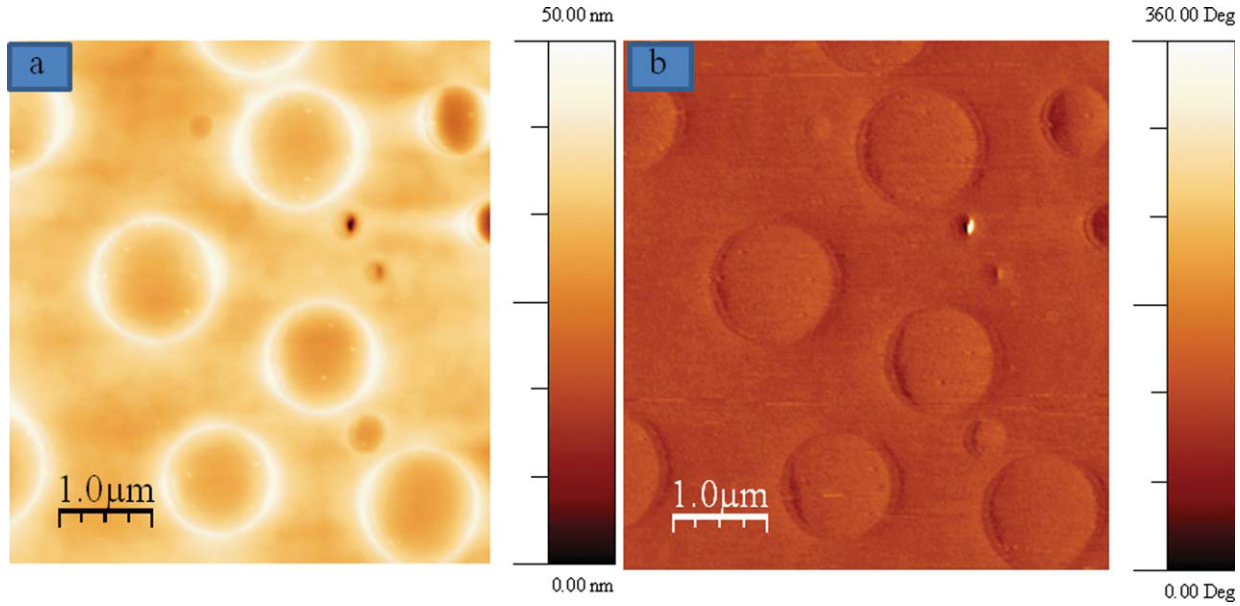

FIGURE 3 Topography (a) and mechanical phase (b) images of sample A (subjected to a heat treatment of 40 °C) taken at room temperature. [Color figure can be viewed in the online issue, which is available at wileyonlinelibrary.com.]

EFM measurements viz. at the center of an island, at a point in between the center and the border of the island (marked red in Fig. 2) and on the matrix (dashed blue ring in Fig. 2) of the polymer blend. By using the ECM previously mentioned, we extracted the value of the dielectric permittivity at these characteristic points for all the samples. The values of the local dielectric permittivity so obtained are given in Table 1.

Table 1 suggests that the center of the islands in the polymer blend treated at 40 °C (sample A) is composed mainly of PVAc as they show a steep increase in their dielectric constant value with increasing the measurement temperature from room (25 °C) to 60 °C. It also shows that the dielectric constant of the matrix is not increasing considerably, which is expected for a PS matrix, as the value of the PS dielectric constant remains essentially unchanged in this temperature range. In general, the blend structure for this sample is like PVAc-rich islands distributed over a PS matrix.

In Figure 6 qualitative images of both topography and dielectric contrast mapping of all the three samples taken at 60 °C

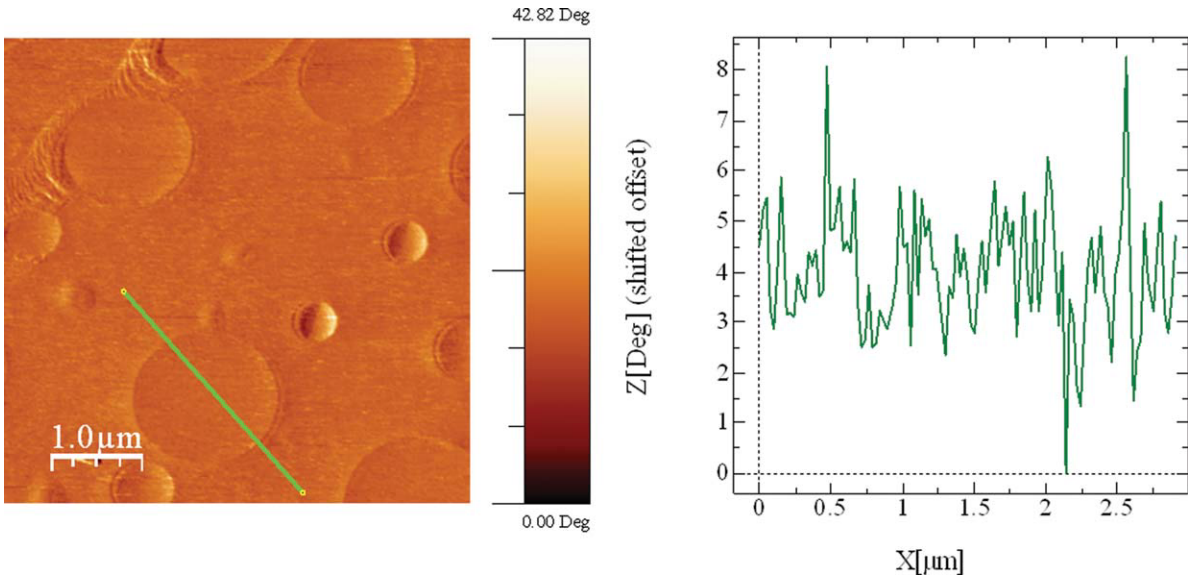

FIGURE 4 Image for the mechanical phase shift of sample A (annealed at 40 °C) (a) and a profile drawn across a PVAc island (b) are shown. The measurement was done at 60 °C. [Color figure can be viewed in the online issue, which is available at wileyonlinelibrary.com.]

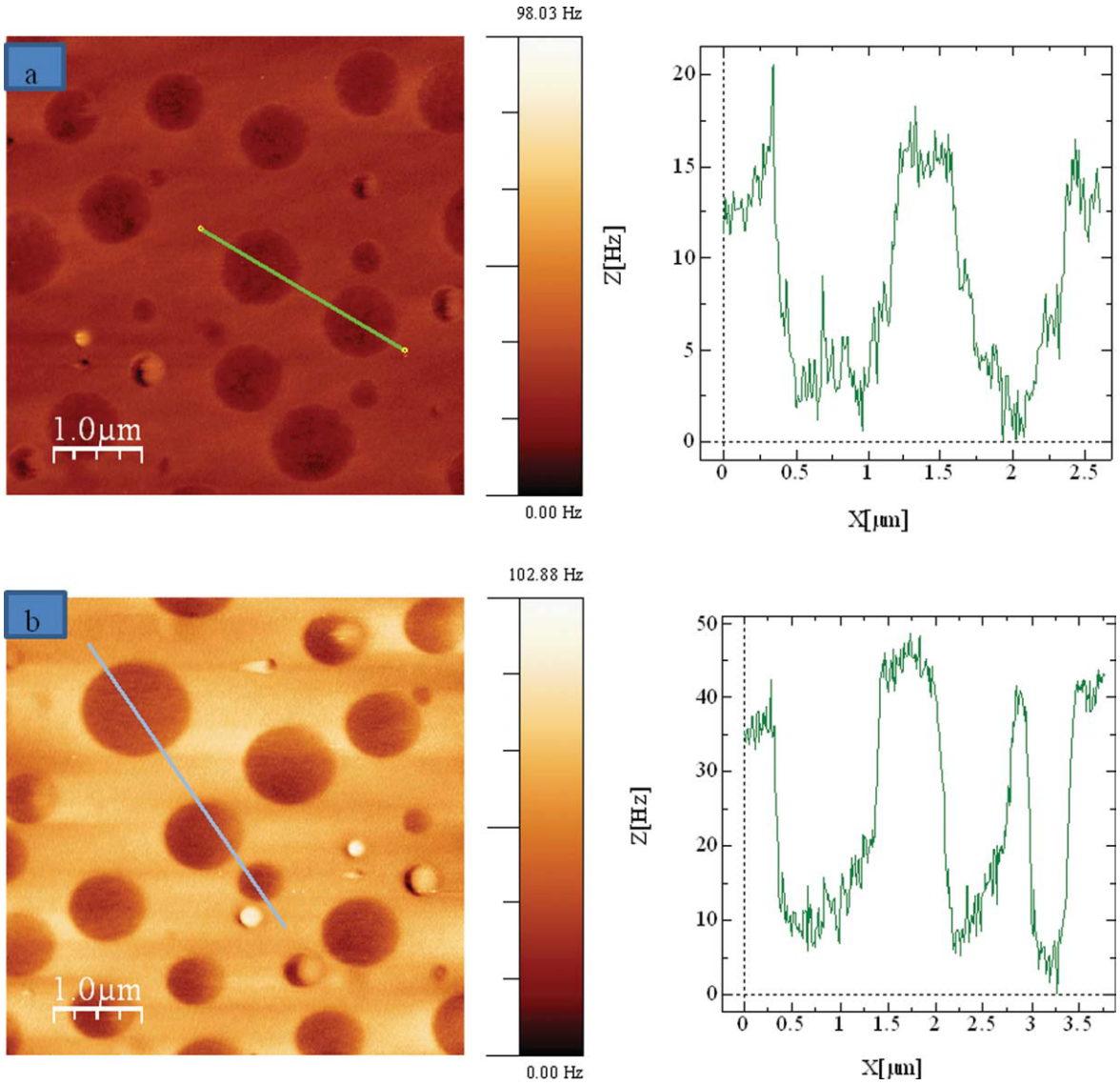

FIGURE 5 Dielectric contrast mapping of the sample annealed at 40 °C, and profiles across PVAc islands are shown both at room temperature (upper row) and at 60 °C (lower row). [Color figure can be viewed in the online issue, which is available at wileyonlinelibrary.com.]

are shown for a better comparison. A careful analysis of Figure 6 shows a continous variation in the shape (topography) of the PVAc-rich islands with respect to thermal treatments. In sample A, the number of islands is large, and they are almost circular in shape with an inward depression, whereas in sample B, which was treated at a temperature (80 °C) well above the glass transition temperature of PVAc (whereas PS is still in glassy state), the number of PVAc

TABLE 1 Values of the Local Dielectric Permittivity for Three Distinct Characteristic Points viz. at the Centre of an Island, at a Point between the Centre and the Border of the Island, and on the Matrix for Samples A and C

	Sample A		Sample C	
Points on the Sample	ε_r 25 °C	ε_r 60 °C	ε_r 25 °C	ε_r 60 °C
Centre of island	3.0±0.3	6±3	2.96±0.45	6.93±3.34
In between centre and border of island	2.3±0.3	4.21±1.40	2.66±0.38	5±2
Matrix	2.31±0.16	2.64±0.56	2.1±0.1	2.12±0.08

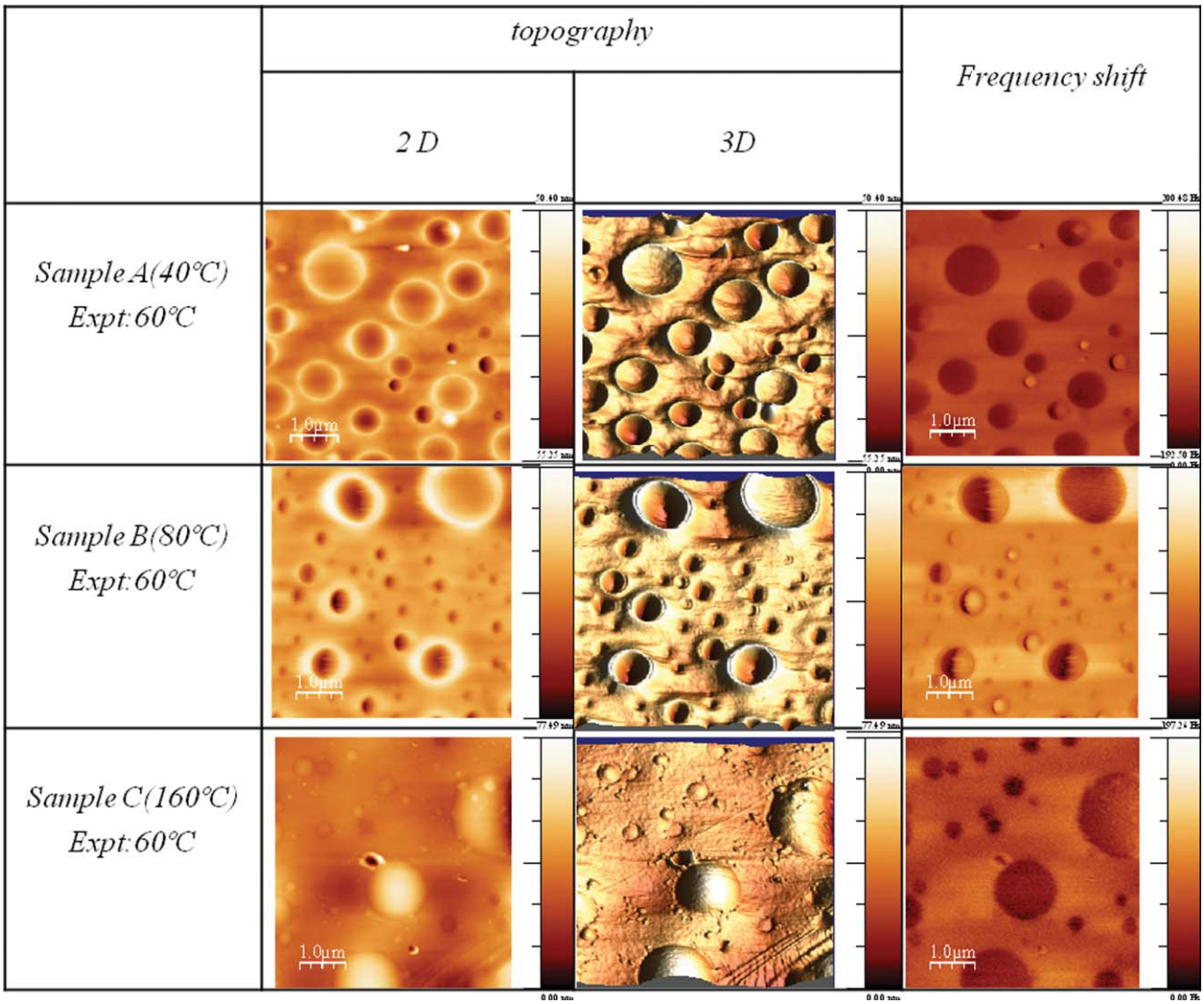

FIGURE 6 The two-dimensional (2D) and 3D images of the topographies and the 2D images of the dielectric contrasts for all the samples are shown. The 3D images of the topographies show continues variation from a large number of smaller depressions (sample A) to a more spherical-like structures (sample C). The scale for the topography reads from 0 to 50 nm, 0 to 55 nm, and 0 to 77 nm for samples A to C, respectively, whereas the scale for the frequency shift is from 0 to 200 Hz for all the three samples.

islands is lower, and with a bigger size, when compared to those of sample A. However, as soon as we increase the temperature above the glass transition temperatures of both polymers, the islands formed by the minority component tends to look more spherical. This evidences the enhanced diffusion of the polymer chains within the blend.

A continous variation in the topography of the polymer blends as the annealing temperature is raised from 40 to 160 °C suggests that the miscibility of the two polymer components could be affected by the thermal treatment. At lower annealing temperature, PVAc chains segregate, but, as these polymer chains are close to their T_g, they cannot migrate far apart, because their mobility is severly restricted. This could explain the values reported in Table 1. The ε_r value at the center of the island is slightly lower than that of pure PVAc; moreover, it is in between that of the PS and PVAc for a point between the center and the border of the island. This suggests that the segregation is not complete, and there could be some PS content within the island. As the annealing temperature is increased above the T_g of the minority component, they achieve greater mobility which in turn facilitate the segregation. This is evident from sample B where PVAc islands are less in number but bigger in size so that it can reduce the interaction with the matrix. When the annealing temperature is well above the glass transition temperatures of both the components, they gain enough mobility to allow eventual full phase separation. This can be investigated by measuring the value of the dielectric permittivity at three characteristic points in sample C as in sample A (Table 1). The increase in the value of dielectric constant at the center and at a point between the center and the border of a PVAc-rich island, and also a decrease in ε_r for the matrix, support the above statements. Moreover, at this aneal-ing temperature PVAc takes a spherical-like shape as a way to reduce the interaction with the PS matrix.

Previous studies on the compatibility of PVAc and PS are consistent with our results. For example, Elashmawi et al.[12] propose that PS and PVAc are compatible with each other. In this case, the samples were prepared by mixing both polymers in acetone and then annealed at 50 °C, which is closer to that used in the preparation of sample A, annealed at 40 °C. On the other hand, Rawal et al.[13] propose that the polymers are partially miscible. Here, they prepared the samples in MEK and then annealed at 70 °C. However, Mamza et al.[14] propose that PS and PVAc are completely immiscible. They investigated the PS/PVAc in the whole composition range, using toluene, MEK, and THF as solvents. All these results suggest that the miscibility of PS and PVAc depends on several factors and in particular, according with our results, immiscibility increases as the annealing temperature is increased. Thus, our results reveal that annealing temperature determines the extent of immiscibility and not only the choices of solvent itself but also when the samples are prepared by spin coating, the effects of the solvents are feeble.

SUMMARY AND CONCLUSIONS

The effect of annealing temperature on the miscibility of PS and PVAc was studied by using EFM technique. EFM allows simultaneous mapping of the mechanical properties (topography + phase) and the dielectric property (frequency shift) of the samples. The local dielectric constant was then quantified using ECM. It is found that, in this way, it is possible to study in detail the different phases in the polymer blend. With this technique, we found that PS and PVAc are thermodynamically immiscible polymers. The previous studies on this system, where conflicting conclusions were obtained, are most probably due to non-equilibrated states arising because of the conditions used for the sample preparation; like different solvents and annealing conditions. However, as far the blends are allowed to evolve to the equilibrium state, our quantitative results show unequivocally that the phase separation becomes nearly complete.

ACKNOWLEDGMENTS

The authors acknowledge the financial support provided by European Union (INFRA-2010-1-1-30 ref: 262348), the Spanish Ministry of Education (code: MAT2007-63681), M. M. acknowledges the Ph.D. grant from the University of the Basque Country (UPV/EHU), Spain.

REFERENCES AND NOTES

1 Polymer Blends: Formulations and Performance; Paul, D. R.; Bucknall, C. B., Eds.; Wiley: New York, **2000**.

2 Guru, G. S.; Prasad, P.; Shiva Kumar, H. R.; Rai, S. K. *J. Polym. Environ.*; DOI 10.1007/s10924-010-0191-2.

3 Kulshreshtha, A. K.; Singh, B. P.; Sharma, Y. N. *Eur. Polym. J.* **1988,** *24*, 33–35.

4 de Gennes, P. G. Scaling Concepts in Polymer Physics; Cornell University Press: London, **1979**.

5 Nishi, T.; Wang, T. T.; Kwei, T. K. *Macromolecules* **1975,** *8*, 227–234.

6 Nose, T. *Polym. J.* **1976,** *8*, 96–113.

7 Davis, D. D.; Kwei, T. K. *J. Polym. Sci. Polym. Phys.* **1980,** *18*, 2337–2345.

8 Bates, F. S.; Wiltzius, P. *J. Chem. Phys.* **1989,** *91*, 3258–3275.

9 Riedel, C.; Arinero, R.; Tordjeman, P.; Ramonda, M.; Leveque, G.; Schwartz, G. A.; de Oteyza, D. G.; Alegria, A.; Colmenero, J. *J. Appl. Phys.* **2009,** *106*, 024315.

10 Riedel, C.; Arinero, R.; Tordjeman, P.; Leveque, G.; Schwartz, G. A.; Alegria, A.; Colmenero, J. *Phys. Rev. E.* **2010,** *81*, 010801.

11 Riedel, C.; Sweeney, R.; Israeloff, N. E.; Arinero, R.; Schwartz, G. A.; Alegria, A.; Tordjeman, P.; Colmenero, J. *Appl. Phys. Lett.* **2010,** *96*, 213110.

12 Elashmawi, I. S.; Hakeem, N. A.; Abdelrazek, E. M. *Phys. B.* **2008,** *403*, 3547–3552.

13 Rawal, H.; Devi, S. *Polym. J.* **1993,** *25*, 1215–1221.

14 Mamza, P. A. A. P.; Folaranmi, F. M. *Eur. Polym. J.* **1996,** *32*, 909–912.

15 O'reilly, J. M. *J. Polym. Sci.* **1962,** *57*, 429–444.

16 Yano, O.; Wada, Y. *J. Polym. Sci A-2.* **1971,** *9*, 669–686.

17 Schwartz, G. A.; Colmenero, J.; Alegria, A. *J. Non-Cryst. Solids.* **2007,** *353*, 4298–4302.

18 Tyagi, M.; Colmenero, J.; Alegria, A. *J. Chem. Phys.* **2005,** *122*, 244909.

19 Girard, P.; Ramonda, M.; Saluel, D. *J. Vac. Sci. Technol. B.* **2002,** *20*, 1348–1355.

20 Riedel, C.; Schwartz, G. A.; Arinero, R.; Tordjeman, P.; Leveque, G.; Alegria, A.; Colmenero, J. *Ultramicroscopy* **2010,** *110*: 634–638.

21 Magonov, S.; Alexander, J. *Beilstein J. Nanotechnol.* **2011,** *2*, 15–27.

22 Horcas, I.; Fernandez, R.; Gomez-Rodriguez, J. M.; Colchero, J.; Gomez-Herrero, J.; Baro, A. M. *Rev. Sci. Instrum.* **2007,** *78*, 013705.

23 NanoScience Instruments. Available at: http://www.nanoscience.com/education/AFM.html. Last accessed on April 28, 2011.

24 Schmitz, I.; Schreiner, M.; Friedbacher, G.; Grasserbauer, M. *Appl. Surf. Sci.* **1998,** *115*, 190–198.